

7-11-2013

Architecture and Design Considerations of Active Antennas on Space Based Platforms

Lupe Romero

Follow this and additional works at: https://digitalrepository.unm.edu/ece_etds

Recommended Citation

Romero, Lupe. "Architecture and Design Considerations of Active Antennas on Space Based Platforms." (2013).
https://digitalrepository.unm.edu/ece_etds/218

This Thesis is brought to you for free and open access by the Engineering ETDs at UNM Digital Repository. It has been accepted for inclusion in Electrical and Computer Engineering ETDs by an authorized administrator of UNM Digital Repository. For more information, please contact disc@unm.edu.

Lupe Romero

Candidate

Electrical and Computer Engineering

Department

This thesis is approved, and it is acceptable in quality and form for publication:

Approved by the Thesis Committee:

Edl Schamiloglu, Chairperson

Christos Christodoulou

Max Light

**Architecture and Design Considerations of Active Antennas on Space
Based Platforms**

By:

Lupe Romero

**B.S. Electrical Engineering
University of New Mexico, 2005**

THESIS

Submitted in partial fulfillment of the
Requirements for the degree of

**Master of Science
Electrical Engineering**

The University of New Mexico
Albuquerque, New Mexico

May 2013

Dedication

I dedicate this work to my wife, Theresa, my children, Aaron, Matthew and Amanda, to my mother, Teodora and to the memory of my father, Audelio. These have been the most important people in my life.

Acknowledgements

I would like to thank my advisor, Edl Schamiloglu, for his advice and guidance.

I would like to thank Max Light at LANL for his advice, his willingness to share his knowledge and for patiently listening to my ramblings.

I would like to thank Christos Christodoulou for serving on my thesis committee.

I would like to thank Dave Smith at LANL for his support of my efforts.

Architecture and Design Considerations of Active Antennas on Space-Based Platforms

By:

Lupe Romero

B.S., Electrical Engineering, University of New Mexico, Albuquerque, 2005

M.S., Electrical Engineering, University of New Mexico, Albuquerque, 2013

Abstract

The design of antennas for space-based applications requires that particular attention be paid to various requirements imposed on the design by the space environment. Additional requirements are driven by the platform on which the antenna will be hosted as well as by the intended use of the antenna, i.e., mission requirements. This thesis provides in depth discussion on the various drivers discussed above and their impact on the design. The thesis provides an antenna design example in order to illustrate how the various requirements drive the final design. The proposed antenna design is intended to provide a certain degree of flexibility such that it can be used on various platforms. Although one of our design goals is flexibility of use, we do need to impose some pseudo-requirements on the antenna in order to provide operational boundaries. As such, our design requirements call for a compact, receive-only antenna design operating in the 20 to 200 MHz frequency range. The optimal solution to meet these requirements is an active antenna.

Table of Contents

List of Figures	viii
List of Tables	ix
Chapter 1	1
1.1 Introduction.....	1
1.2 Primary SV Requirement Driver.....	2
1.3 Secondary SV Requirement Driver.....	3
1.4 Prime Real Estate.....	4
1.5 Small Satellites.....	5
1.6 Antenna Specific Concerns.....	6
1.7 Intertwined Driver Behavior	7
1.8 Organization of This Thesis.....	8
Chapter 2.....	9
2.1 Environmental Drivers.....	9
2.2 Thermal.....	9
2.3 Vibration	10
2.4 Radiation.....	10
2.5 Ionospheric Impacts	11
2.6 Summary of Chapter 2.....	12
Chapter 3.....	13
3.1 Antennas	13
3.2 Antenna Performance Parameters.....	13
3.2.1 Antenna Directivity.....	14
3.2.2 Antenna Gain	15
3.2.3 Radiation Pattern.....	16
3.2.4 Radiation Resistance.....	18
3.3 Antenna Variety	18
3.4 Summary of Chapter 3	19
Chapter 4.....	20
4.1 Active Antenna Design	20
4.2 Advantages of Active Dipole for Space.....	21
4.2.1 SWaP Considerations In General.....	21

4.2.2	Size and Weight	22
4.2.3	Power	22
4.3	Proposed Active Antenna Solution	22
4.3.1	Elements	23
4.3.2	Amplifier	24
4.4	Summary of Chapter 4	25
Chapter 5	26
5.1	Design Implementation	26
5.2	Element Design	26
5.2.1	Model	27
5.2.2	Element Implementation	36
5.3	Amplifier and Balun PCB Design	37
5.3.1	PCB Implementation	44
5.4	Housing Design	45
5.5	Summary of Chapter 5	49
Chapter 6	50
6.1	Test and Verification	50
6.1.1	Amplifier Measurements	50
6.1.2	Antenna Gain Measurements	51
6.2	Summary of Chapter 6	54
Chapter 7	55
7.1	Conclusions	55
7.1.1	Scaling	55
7.2	Path Forward	56
References	57

List of Figures

Figure 1. Artist's rendition of a GPS block IIF satellite.....	4
Figure 2. Examples of cube sats.	5
Figure 3. Representation of intertwined driver behavior.....	7
Figure 4. A 3-D radiation pattern.....	17
Figure 5. A 2-D vertical plane radiation pattern.	17
Figure 6. Dipole element model in the 4NEC2 simulations.....	28
Figure 7. 3D dipole pattern at 20 MHz (modeled).	29
Figure 8. Dipole current distribution at 20 MHz (modeled).....	29
Figure 9. 3D dipole pattern at 110 MHz (modeled).....	30
Figure 10. Dipole current distribution at 110 MHz (modeled).	30
Figure 11. 3D dipole pattern at 200 MHz (modeled).....	31
Figure 12. Dipole current distribution at 200 MHz (modeled).	31
Figure 13. Vertical plane radiation pattern, $f(\theta)$, at 20 MHz (modeled).	32
Figure 14. Vertical plane radiation pattern, $f(\theta)$, at 110 MHz (modeled).....	33
Figure 15. Vertical plane radiation pattern, $f(\theta)$, at 200 MHz (modeled).....	34
Figure 16. Modeled gain at $\phi = 0$ and $\theta = 90$	36
Figure 17. Reflection efficiency at various impedance transformations as a function of frequency.	38
Figure 18. Dipole gain as a function of reflection efficiency and frequency.....	39
Figure 19. LPA and dipole bandwidth comparison, (gain as a function of frequency). ...	40
Figure 21. Schematic of the LNA with balun.	43

Figure 22. Layout artwork for the LNA PCB.	44
Figure 23. Photograph of the prototype LNA assembly.	44
Figure 24. Photograph of the prototype active dipole installed in the prototype housing.	45
Figure 25. Photograph of the full size prototype active dipole antenna.	46
Figure 26. Photograph of the active dipole antenna.	46
Figure 27. Drawing of the proposed EDU housing.	47
Figure 28. Drawing of the proposed EDU housing with cover.	48
Figure 29. Drawing of the proposed EDU active dipole.	49
Figure 31. Measured completed active antenna gain as a function of frequency.	53

List of Tables

Table 1. Dipole 3 dB BW's (modeled).	33
Table 2. Dipole radiation resistance (modeled) as a function of frequency.	35
Table 3. LNA MMIC S-parameters.	41
Table 4 LNA gain (measured) as a function of frequency.	50
Table 5 Calculated far field distances as a function of frequency.	52

Chapter 1

1.1 Introduction

Space-based platforms present a variety of interesting challenges in regards to the design and operation of the instruments which they host. The instruments of particular interest in this thesis are the antennas that are hosted on space-based platforms, or space vehicles (SVs). Antennas are essential for communication and data collection but can present several challenges when integrated onto a SV. Many of the antenna-related challenges can be addressed through the use of active antenna configurations.

An active antenna is comprised of an antenna element or elements, of some type, and active amplification circuitry integrated into one assembly. Active antennas can be configured as transmit or as receive antennas, depending on the configuration and placement of the amplifier circuitry.

The use of amplification in close proximity to the antenna elements lends flexibility to the design by providing signal gain immediately upon receiving or immediately prior to transmitting a signal. This enhancement in signal gain can often be used to offset the diminished gain response of less than ideal antenna elements and to improve the system signal-to-noise ratio in the case of a receiving antenna [1]. An example of a less than ideal antenna element would be one that is physically small relative to the length of a resonant non-active antenna element.

The ability to meet performance requirements with a physically smaller antenna is one of the primary attributes that make an active antenna attractive for use on space platforms, where physical space is limited.

1.2 Primary SV Requirement Driver

Design of instrumentation for a space-based application requires working against several requirements and boundaries imposed by the space vehicle. Additionally, these requirements are not necessarily the same for every vehicle and are primarily driven by its particular mission.

An SV's mission is defined as its purpose or intended use. Mission parameters can vary greatly from one mission to another, just as mission types can differ significantly. Mission types can be scientific, military, intelligence-gathering, educational, and commercial [2], or some combination of these. For the purposes of this thesis the mission type will be an unmanned, earth-orbiting, scientific mission.

Categorization can be further refined by specifying anticipated mission duration and particular orbital trajectory. Mission duration and orbital trajectory are dependent on the type of scientific data being collected and the selected location for observation [2]. Mission duration is driven by the amount of time required to adequately study the phenomenon of interest. Orbital trajectory is selected to provide the optimal location in terms of orbit altitude and type.

1.3 Secondary SV Requirement Driver

As stated previously, the primary driver influencing instrument design, as well as design of the vehicle, is the mission. However, there are significant secondary drivers that must be considered. Chief among these is the cost and its relation to the allotted budget. The realities of limitations on funding, whether it is from public or private sources, along with the high cost of space related components and processes, require that execution of the mission be accomplished as economically as possible.

The space-flight trinity of size, weight and power (SWaP) are the ever-present drivers influencing the design of instrumentation for space and are a direct consequence of the aforementioned budgetary constraints. The size and weight requirements are closely coupled, as instrument weight is usually a direct function of its size. Size and weight are of prominent importance mainly due to the high cost of launching an SV into space. These costs can range from tens to hundreds of millions of dollars per launch.

The power requirement becomes more critical after launch when the vehicle and instrumentation begin operation. The power budget allotted for completion of the mission must be considered early in the design stage of the instruments as well as the vehicle. The sources of operational power are either from storage that is launched with the vehicle or from methods of generation when in operation. Commonly, it is a combination of the two with the storage element being rechargeable batteries and the generating element being solar panels, for example [2].

1.4 Prime Real Estate

The high costs described above make physical space on the vehicle, in terms of available mounting surfaces, extremely valuable. One approach that is used to take advantage of the available space is to host secondary payloads aboard the SV. One example of this is the secondary payload hosted aboard GPS satellites. The primary GPS mission is to support terrestrial navigation for both civilian and military use. A secondary mission is the United States Nuclear Detection System, USNDS, monitoring mission, which is also hosted on the GPS vehicles.



Figure 1. Artist's rendition of a GPS block IIF satellite.

Figure 1 is a depiction of a GPS satellite. Multiple antennas can be seen on the earth-facing side of the vehicle. This view provides a good example of the limited space available and the need to take advantage of this space through concentration of instruments - in this case it is antennas.

This is an example of a government payload hosted on a government SV. However, there is a trend that is gaining popularity where government payloads are secondary payloads on commercial space vehicles [3].

1.5 Small Satellites

Another approach for countering the high conventional launch cost is to use smaller satellites. This method allows for deployment of multiple satellites, also known as multiple manifest, from a single launch vehicle. Additionally, smaller SVs do not require the larger, and therefore, more expensive launch vehicles. They can be launched from other platforms such as high altitude conventional aircraft, such as Orbital's Stargazer launch aircraft [2].

The trend to smaller satellites is gaining momentum, with the ever-increasing use of nano-satellites, such as the cube sat. Examples of cube sats can be seen in Figure 2 [4,5].

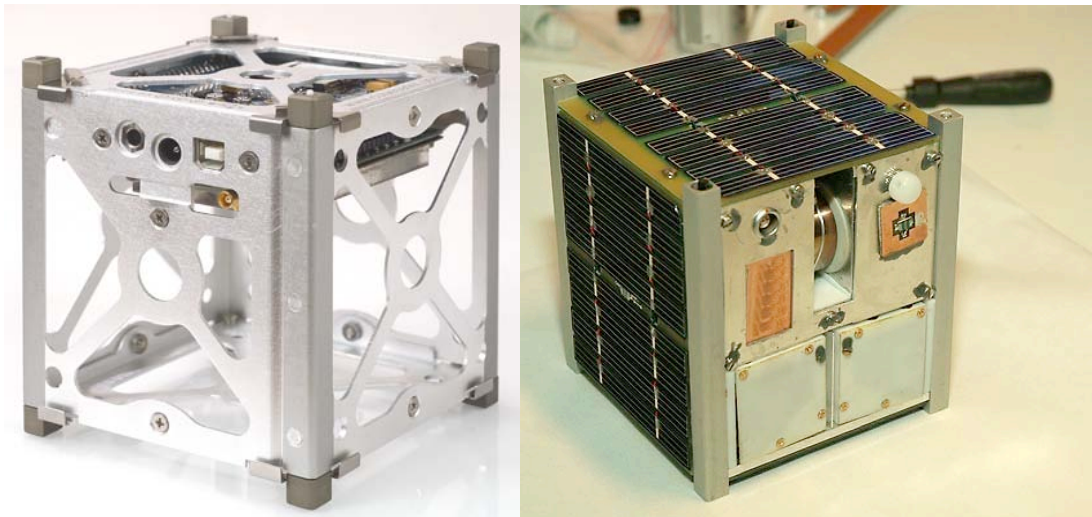


Figure 2. Examples of cube sats.

Cube sats are becoming very popular due to their low development and launch costs. Miniaturization of electronic components and increased capability in Field Programmable Gate Arrays, FPGAs, allow for hosting miniature instrumentation with greater performance capability.

1.6 Antenna Specific Concerns

Antenna designs fall victim to the SWaP concerns described above. The size requirements are usually of greatest concern due to the nature of the antenna elements and the relationship between their physical size and their ability to capture or transmit sufficient signal power, relative to the wavelength(s) of the signal of interest [6,7]. Again, size and weight are very closely coupled, with larger antenna elements being necessarily heavier than smaller ones.

The proximity of the antenna to the vehicle can have a significant influence on the antenna pattern, causing pattern distortion, and may require a boom or some other type of extending mechanism to provide distance between the antenna and the vehicle. This adds both weight and complexity to the antenna design. It is common for both the antenna elements and boom, if required, to be in a stowed configuration during launch and then deployed when in space. This results in additional complexity of design and risk to proper deployment.

In the case of a non-active antenna, continuous power consumption is of no concern. However, the amplification element of an active antenna design will consume power and

must be considered. An additional source of antenna-related power consumption would be the deployment mechanism used for the elements or boom, if used.

1.7 Intertwined Driver Behavior

The various drivers discussed have an influence on one another. The size of an instrument can affect its weight. The mission's signal frequency band of interest and operation affect the design of the instrumentation and the antennas. The design of the instrumentation and antennas affect power requirements. Power consumption affects design and configuration of the power source. All of these, in turn, affect and are affected by the allocated financial budget. The dominant driver should be the mission, with tradeoffs between the other drivers maintaining the mission within budget.

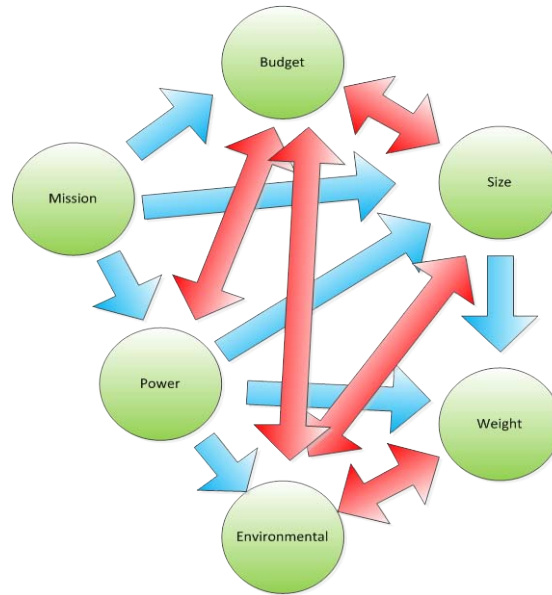


Figure 3. Representation of intertwined driver behavior.

1.8 Organization of This Thesis

This thesis presents the result of research performed to examine the viability of a simple active dipole antenna that will meet the need for a receive antenna to be used on space based platforms.

The remainder of this thesis is organized as follows. Chapter 2 describes the various environmental drivers that are encountered in space based applications and influence the design of the antenna. Chapter 3 is a discussion of basic antenna characteristics and functional parameters. The discussion provides the background information required for the remainder of the thesis. Chapter 4 describes an active antenna and its merits relative to a space based application. Chapter 5 describes the particular design that is the subject of this thesis. The discussion includes details on the implementation of the design. Chapter 6 presents the results of the tests and measurements performed on the antenna. Finally, Chapter 7 presents the conclusion of the research and presents a path for future or continued research.

Chapter 2

2.1 Environmental Drivers

The launch and post-launch (i.e., space) environment is far from benign. The SV and its payload can experience extreme changes in environmental variables, such as temperature, atmospheric pressure, and background radiation. Additionally, the SV can experience extreme mechanical vibrations and mechanical shock created during launch and on orbit deployment. These environmental extremes have a profound impact on system reliability and lifetime, due to both one-time stresses and long term, accumulated exposures.

2.2 Thermal

The SV can experience extreme changes in temperature during launch. This is due to the change in temperature as a function of altitude. During launch, these changes can occur within a short span of time, as the launch vehicle quickly passes through the various layers of the atmosphere [2].

The thermal challenges continue when the vehicle reaches space and becomes operational. The absence of atmosphere and extremely low pressure (close to vacuum) in space means that any heat generated by instrumentation must be dissipated through conduction, as there is no mechanism for heat transfer through convection. Thermal variations must be considered during the initial design of the SV and instrumentation. The mechanical design influences the dissipation of heat while the electrical design influences the generation of heat.

2.3 Vibration

The SV and on-board instrumentation experience various types of vibration during launch. The primary forces influencing these vibrations are changes in air pressure and mechanical reverberations during launch and ascent. The typical launch vehicle, i.e., rocket, is powered by large liquid or solid fueled engines. The operation of these engines, as well as the operation of all associated mechanical support assemblies, e.g., turbo-pumps, produces mechanical vibration throughout the launch vehicle [2]. During the initial ascent phase of the launch, the vehicle passes through an atmosphere of varying pressure and density at a high rate of speed. This passage produces additional vibrations, induced by both mechanical reverberation and the acoustics related to airflow over the vehicle. The main types of vibrations experienced by the vehicle are sinusoidal vibration, which is sustained within a narrow frequency band, random vibration, which is spread over a broad range of frequencies, and acoustic vibration, which is primarily driven by pressure changes and reverberations during launch and flight through the atmosphere [2].

2.4 Radiation

The space environment is rich in sources of radiation. Of particular concern for space-based instrumentation are the high energy phenomena that can cause damage to electronic components. These radiation sources include high energy electrons, high energy protons, solar particles, galactic cosmic rays, and x-rays. The type of radiation source encountered and its energy level is dependent on the particular location of the SV,

that is, altitude and orbit. For example the Van Allen radiation belts pose a significant risk to instrumentation due to the high energy electrons and ions they contain [2].

The effects of radiation on instrumentation can range from single-event upsets, which are single or multiple bit disruptions of data, to permanent damage to the internal structure of components. Damage caused by radiation can manifest immediately following exposure or can appear much later as a result of accumulated dosage. The severity of the effect depends on the type and energy level of the particle. The effects of radiation on instrumentation can be combated through the use of shielding material and selection of radiation hardened components.

2.5 Ionospheric Impacts

The ionosphere is a layer of the earth's atmosphere comprised of charged particles in the form of free-electrons and ions. The ionization is caused by solar UV and X-ray radiation [2]. An ionized or charged-gas region is known as plasma [8]. The electron and ion density of the ionosphere, and therefore the plasma, varies as a function of solar activity, the earth's day and night cycle as well as altitude.

The primary impacts of the ionosphere on space vehicles and instrumentation are electrostatic charge accumulation and subsequent electrostatic discharge (ESD) and its effect on electromagnetic signal propagation between the vehicle and earth.

An ESD event poses some risk to electronic components within an instrument. However, a discharge path must exist between the origin of the discharge and the ESD sensitive component(s). An ESD produces an EMP signal which can be detected by RF receivers so that ESD can be a source of interference.

Electromagnetic waves interact with the ionosphere and this interaction is described through a dispersion relation, which governs their propagation through the plasma [8]. The electromagnetic dispersion relation exhibits a cutoff behavior. That is, there exists a critical electron density, n_c , at which the frequency of the propagating EM wave, ω , is equal to the plasma frequency, ω_p . Propagating EM wave whose frequencies are equal to or below ω at cutoff will not propagate through the plasma [8]. The plasma frequency is related to the electron density through Eq. (1),

$$\omega_p = \sqrt{\frac{n_c e^2}{\epsilon_0 m_e}}, \quad (1)$$

where e is the electron charge, m_e is the electron mass, and ϵ_0 is the permittivity of free space. The average value of the cutoff frequency is 40 MHz.

2.6 Summary of Chapter 2

Chapter 2 presented the major environmental characteristics that influence the design of the antenna or any other electronic instrumentation intended for use in space. From the information presented, it is evident the launch and on-orbit environment are both harsh and present challenges to the design.

Chapter 3

3.1 Antennas

The basic definition of an antenna is that it is an electrically conducting device for transmitting and receiving radio waves [6,7]. This is a fundamental and accurate definition, but it does not adequately convey the underlying complexity in function, and variation in form, of antennas.

There are many antenna parameters that must be considered in the selection of an antenna for a particular application, the primary one being the frequency range of operation. In addition to this are the desired radiation pattern, required gain, directivity, and polarization. These are the main performance parameters of interest. However, there are other parameters that must be considered. These are size, weight, mechanical configuration, power requirements, interface connections, and mounting. All parameters, both performance specific and others, must be carefully considered during design. The difficulty of this task is compounded when the application is space vehicle-based. The SV and space-related drivers discussed in the previous Chapters must be factored into the design.

3.2 Antenna Performance Parameters

The antenna frequency range of operation is probably the most critical driver of the antenna design. This is due to the relationship between frequency or wavelength and the physical dimensions of the antenna elements. The wavelength, λ , is a function of the frequency and the velocity of propagation of the wave [6,7], and is given by Eq. (2),

$$\lambda = c/f, \quad (2)$$

where

$c = \text{speed of light}$

$f = \text{frequency.}$

The frequency typically specified for an antenna is the center of the frequency band of interest or the frequency at the center of the intended range of operation. Frequency bandwidth is the width of this range of operation

$$BW = f_2 - f_1.$$

A narrow band antenna is one with a limited frequency range of operation while a broadband antenna has a wide frequency range of operation. The bandwidth of the antenna provides the first layer of filtering or frequency selection for the receiver system.

3.2.1 Antenna Directivity

Directivity is a measure of an antenna's radiation intensity in a given direction relative to the radiation intensity of an isotropic radiator averaged over all directions [6,7], given by Eq. (3),

$$D = U/U_0, \quad (3)$$

where

$D = \text{Directivity}$

$U = \text{radiation intensity (in a given direction)}$

$U_0 = \text{radiation intensity of isotropic source.}$

3.2.2 Antenna Gain

Antenna gain is similar to antenna directivity; however, gain takes into account the antenna's radiation efficiency. Both gain and directivity are functions of the observation angles, θ and Φ , [1,6,7], and are related through Eq. (4)

$$G = e_{cd}D \quad (4)$$

$D = \text{Directivity}$

$e_{cd} = \text{radiation efficiency.}$

Radiation efficiency is a measure of how much power is delivered to the load relative to how much power is lost due to conductive and dielectric properties of the antenna [6,7].

Radiation efficiency is defined as,

$$e_{cd} = R_r / (R_r + R_l) \quad (5)$$

where

$R_r = \text{Radiation resistance}$

$R_l = \text{loss resistance.}$

Absolute antenna gain is a quantity that not only takes into account the radiation efficiency, but also the reflection, or mismatch efficiency, e_r . Therefore, absolute or total antenna gain is defined as [1,6,7]

$$G_{abs} = e_{cd}e_rD = e_0 D, \quad (6)$$

where

$$e_0 = e_{cd}e_r \quad (7)$$

with

$$e_r = (1 - |\Gamma|^2) \quad (8)$$

and with the reflection coefficient, Γ , defined as [9]

$$\Gamma = (Z_{in} - Z_0)/(Z_{in} + Z_0). \quad (9)$$

Here Z_{in} is the input impedance of the antenna

with

$$Z_{in} = R_a \pm X_a \quad (10)$$

$R_a = \text{Antenna resistance}$

$X_a = \text{Antenna reactance}$

and Z_0 is the characteristic impedance of the load.

3.2.3 Radiation Pattern

An antenna pattern is a graphical, or mathematical, representation of the radiating properties of an antenna with respect to three-dimensional spatial coordinates [7]. The graphical representation can convey qualitative and quantitative information about the directivity, gain, and radiation intensity. A sample of a 3-D antenna pattern and a 2-D

vertical plane pattern, both generated using the 4NEC2 modeling software [10], can be seen in Figures 4 and 5.

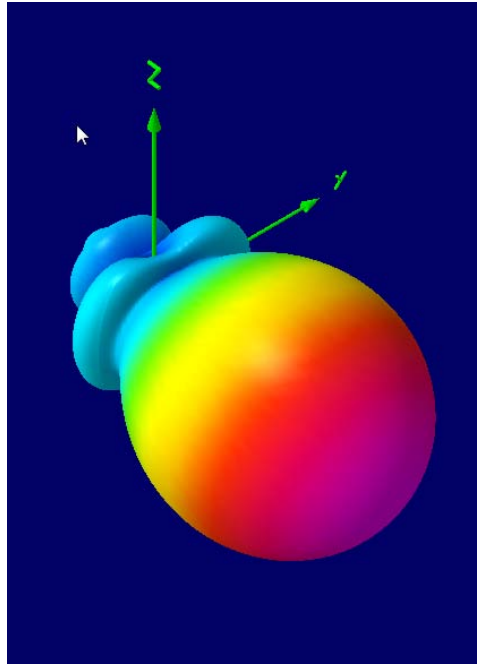


Figure 4. A 3-D radiation pattern.

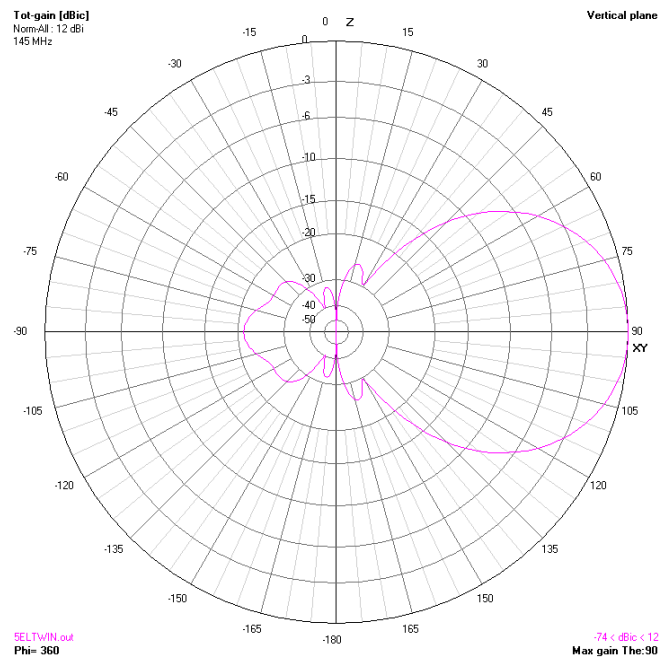


Figure 5. A 2-D vertical plane radiation pattern.

This particular example is of a highly directional, multi-element antenna. The plots show a concentration of radiated energy in the +X direction. This indicates high directivity and likely high gain, depending on efficiency.

3.2.4 Radiation Resistance

Radiation resistance is the apparent resistance of the antenna as seen by the load it is connected to. It is not a resistance within the physical antenna elements, i.e., loss resistance, but rather is the quantity that couples the antenna terminals to radiating space [7].

Radiation resistance is the resistive component of the input impedance Z_{in} as given in Eq. (10). That is,

$$R_r = R_a. \quad (11)$$

3.3 Antenna Variety

There are a multitude of antenna designs, architectures and configurations available. The variation in antenna designs is driven by several factors. The intended use of the antenna, the frequency of operation, and the location of installation all factor into the design.

Antenna architectures can range from simple wire type antennas to more sophisticated aperture types. They can be constructed of distinct, three dimensional protruding

elements or planar copper patches fabricated as a printed circuit board. Antennas can be simple single element devices or complex arrays [6,7].

Antennas can be designed with a particular wave polarization scheme in mind. That is, the polarization can be linear, elliptical, or circular. The circular and elliptical categories can be further divided into right or left hand polarizations. This variety means that most performance requirements can be achieved with one configuration or another.

3.4 Summary of Chapter 3

Chapter 3 provided important background information on antennas. A basic definition of an antenna was provided and several fundamental antenna parameters were presented. The material presented in general terms in this chapter, will be applied to the actual design in Chapter 5.

Chapter 4

4.1 Active Antenna Design

The pseudo-requirements for the antenna studied in this thesis indicate that this is a receive-only antenna operating in the 20 MHz to 200 MHz frequency range. The antenna design of choice to meet this requirement is an active dipole design. This design offers many benefits, as will be discussed, but its primary advantage is simplicity and flexibility. The active dipole can be configured to fit many varied applications. This is due in a large part to the characteristic of an active antenna that allows for the use an electrically small antenna element, relative to the wavelength of interest. In addition to this is the use of a dipole element configuration, which provides an omni-directional pattern [6,7].

The active portion of the antenna provides immediate amplification of the incoming signal. This amplification can provide compensation for diminished signal amplitude that may result from antenna elements that are not of optimum length for the frequency of interest.

An omni-directional pattern is one that exhibits low directivity, producing a pattern that is relatively uniform as a function of the spatial coordinates θ and Φ for a given band of wavelengths, and therefore frequencies, around the $\lambda/2$ resonant length. The omni-directional pattern provides an extremely broad field of view for the antenna, making the dipole a good general purpose antenna. A dipole is a linearly polarized antenna.

4.2 Advantages of Active Dipole for Space

The active dipole has many desirable attributes that address the various challenges presented by the various space related drivers discussed previously. The ability to achieve acceptable gain and a wide field of view, i.e., a broad pattern in a compact, uncomplicated unit makes this antenna a good choice for a wide variety of applications. The relatively small size means that the antenna will take up little physical space in the SV. The simple architecture of the dipole elements provides an uncomplicated configuration that is easier to deploy relative to complex multi-element arrays, or reflector type antennas. The simple amplifier printed circuit board, PCB, is mechanically robust and will perform well in the vibration environment. The power consumed by the amplification circuit is low in relation to the enhanced signal amplitude that is gained.

4.2.1 SWaP Considerations In General

A simple design that meets performance requirements is preferred for space-based applications. Complexity of design can add risk to any space based mission, particularly in the areas of deployment and post deployment operation. A complex design will typically have an adverse effect on the SWaP budget. A complex design is typically larger in size and, therefore, heavier. The impact on power is more difficult to determine as it requires a detailed description of the complexity and implementation of the specific design being considered. In general, a non-active design will not require power for amplification, but will consume some finite amount of power during deployment.

4.2.2 Size and Weight

The proposed design will consist of a $\lambda/2$ dipole, configured for the center frequency, f_0 , of the band of interest. After deployment, the antenna elements will be the largest part of the antenna. The volume envelope taken up by the antenna is a product of the width and depth of the housing multiplied by the length of the antenna elements. The small size of the PCB, the tubular elements, and the composite housing are all lightweight components. This provides for an overall low weight for the completed assembly.

4.2.3 Power

The only active component in the amplifier circuit is the amplifier. The remaining components are the passive biasing and matching components. Thus, the amount of power drawn by the active antenna is low. The mechanism for deploying the elements will draw power, but this will be a one-time event.

4.3 Proposed Active Antenna Solution

The antenna design is that of a 20 MHz to 200 MHz (bandwidth of 180 MHz) dipole coupled to an RF amplifier. The antenna elements will be of length $\lambda/2$ at the center frequency, f_0 . The elements will be hollow metallic tubes that will be secured to a non-conductive housing. A balun transformer will be used to couple the balanced antenna elements to the unbalanced transmission line feeding the RF amplifier. The output of the amplifier is connected to a 50Ω RF connector.

4.3.1 Elements

The center frequency of the antenna will be

$$f_0 = f_1 + \frac{f_2 - f_1}{2}, \quad (12)$$

where

$$f_2 = 200 \text{ MHz}$$

$$f_1 = 20 \text{ MHz.}$$

Therefore, $f_0 = 110 \text{ MHz}$.

The antenna elements are resonant, from a $\lambda/2$ dipole perspective, at the center of the frequency band as discussed above. However, the antenna will appear electrically small at the low end of the frequency band, where it is approximately a $\lambda/10$ dipole [6,7]. The antenna will be approximately a full wavelength, λ , at the upper end of the frequency range.

The directivity of the antenna elements will not vary significantly over the low to slightly above mid-band frequency range. Changes in directivity will become more apparent at the upper end of the frequency band [6,7] where the element length approaches λ .

The radiation resistance of the antenna will vary greatly over the frequency range. The radiation resistance of the dipole antenna will be small at the low end of the frequency band and higher at the high end of the band. This characteristic of the radiation resistance will have an effect on efficiency, and therefore, on the gain.

4.3.2 Amplifier

A low noise amplifier, LNA, is required for this application. The active antenna is the first component, of a longer signal receiver chain. The overall noise figure, NF, of the cascaded system is dominated, or 'set', by the noise figure of the first component, F_1 , in the signal processing chain [11,12].

$$NF = F_1 + \frac{F_2-1}{G_1} + \frac{F_3-1}{G_1G_2} + \dots + \frac{F_n-1}{G_1G_2G_3\dots G_n} \quad (13)$$

In Eq. (13) the $G_1\dots G_n$ variables represent the gain of the various links in the signal receive chain and the $F_1\dots F_n$ variables represent the noise factors of the various signal chain links.

Further, the stability of the LNA must be assured to prevent spurious signal generation and oscillations. The stability of the amplifier is assessed by examination of the S-parameters using the stability criteria $k > 1$ and $|\Delta| < 1$ [11],

where

$$k = \frac{1 - |S_{11}|^2 - |S_{22}|^2 + |\Delta|^2}{2|S_{12}S_{21}|} \quad (14)$$

and

$$\Delta = S_{11}S_{22} - S_{12}S_{21}. \quad (15)$$

Here the S-parameters are defined as the scattering parameters of a two port network [11]. That is, the S-parameters provide the reflection and transmission coefficients for the

two port network, which in our application is the amplifier. The individual S-parameters are defined as follows:

S_{11} = *Input reflection coefficient*

S_{22} = *Output reflection coefficient*

S_{21} = *Forward transmission coefficient*

S_{12} = *Reverse transmission coefficient.*

The amplifier will have a moderate amount of signal gain. The primary purpose of the amplifier gain is to compensate for the lower off-resonance gain of the antenna elements and transmission line loss between the antenna and receiver.

4.4 Summary of Chapter 4

In Chapter 4 the description of an active antenna was presented. The various components of an active antenna were detailed and the merits of such a design were discussed. The elements of the proposed design were presented along with the anticipated performance characteristics for each component.

Chapter 5

5.1 Design Implementation

The completion of the antenna design was approached in a two-stage fashion. Initially, a prototype version of the antenna was built. The fabrication of a prototype allows for test and validation of the design using a lower cost antenna that is functionally analogous to the desired final product. The second stage in the design process is to move ahead with the building of an engineering design unit, EDU, and subsequent flight unit.

5.2 Element Design

The antenna architecture of choice is a $\lambda/2$ dipole resonant at a frequency of 110 MHz, which results in a total element length of 1.4 meters calculated from:

$$\frac{\lambda}{2} = \left(\frac{c}{f}\right)/2 \quad (16)$$

where

$c = 3 \times 10^8$ meters per second (*speed of light in vacuum*).

The selection of a single $\lambda/2$ dipole at the center frequency imposes a limit on the bandwidth of uniform gain as a function of frequency. Using a multi-element, log periodic array of dipoles, or other more complex elements, provides improved bandwidth performance; however, addition of elements increases the overall size and complexity of the design.

The log periodic antenna design requires that a specific relationship be maintained relative to the length and spacing of the individual antenna elements [1,6,7]. The placement of elements at the edges of the frequency band, in addition to the element at the center, improves bandwidth but results in extremely long feeder lines (rods) and large low end elements. The ‘outer’ elements can be moved in (in terms of frequency) from the band edges, thus decreasing the overall antenna size while still gaining bandwidth relative to a single element, however, this size is still large compared to the single element design. Another alternative is to deviate from the true log periodic architecture and simply implement a 3-element array of $\lambda/2$ dipoles, with no consideration to the required log periodic spacing.

Improved bandwidth performance is definitely possible using more complex antenna elements, however, the intent of the thesis is to provide a simple, compact, antenna design. Additionally, multiple elements necessarily require multiple deployment mechanisms, which add complexity to the design. In space based applications, any increase in complexity is an increase in risk; in this case risk of non-deployment of an element.

5.2.1 Model

The dipole antenna was modeled using the 4NEC2 antenna modeling software [10]. The dipole model is constructed of 41 wire segments. The signal source is connected to the center segment. The active antenna is a receive-only design; however, the model treats

the antenna as a transmitting antenna. This is a valid method based on the property of reciprocity of antenna radiation patterns [6,7].

The 4NEC2 antenna model is shown in Figure 6 below. The dipole element is aligned along the z axis. The point of observation for the modeled pattern is at $\theta=90$ and $\Phi=0$.

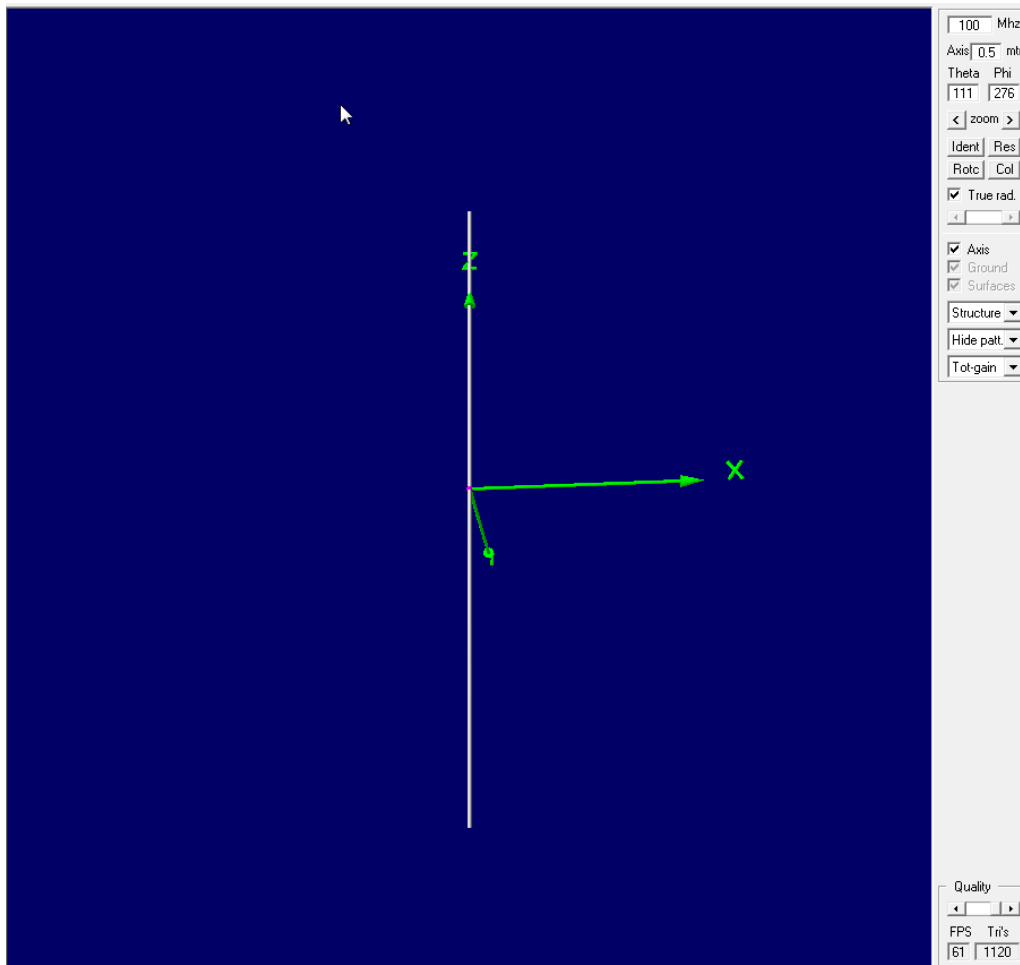


Figure 6. Dipole element model in the 4NEC2 simulations.

Three dimensional antenna patterns and current distributions at $f= 20$ MHz, $f =110$ MHz and $f=200$ MHz are shown in Figures 7 through 12.

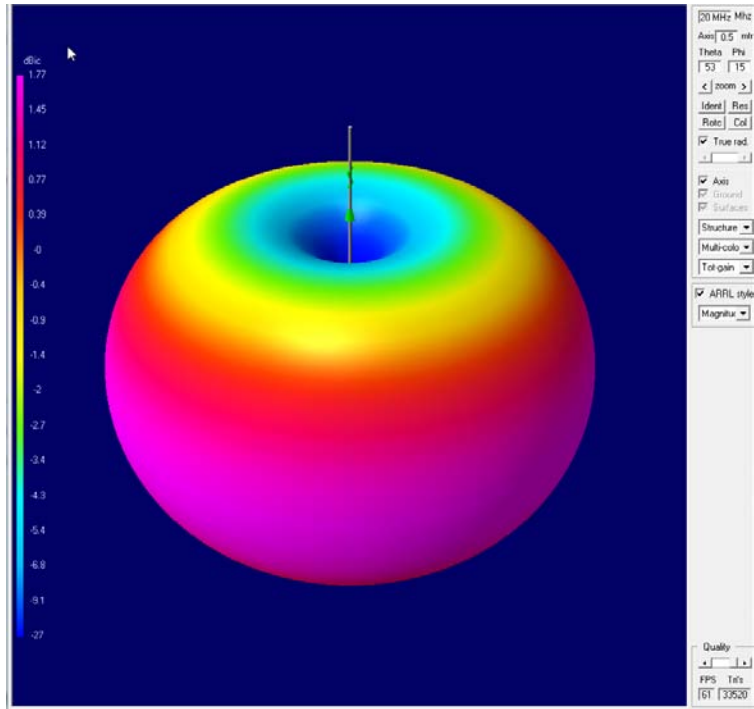


Figure 7. 3D dipole pattern at 20 MHz (modeled).

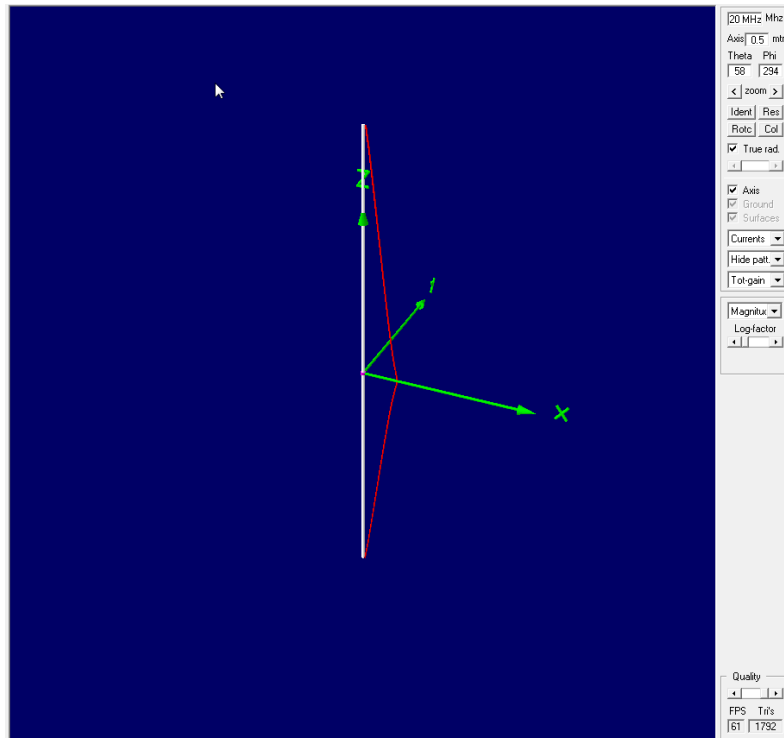


Figure 8. Dipole current distribution at 20 MHz (modeled).

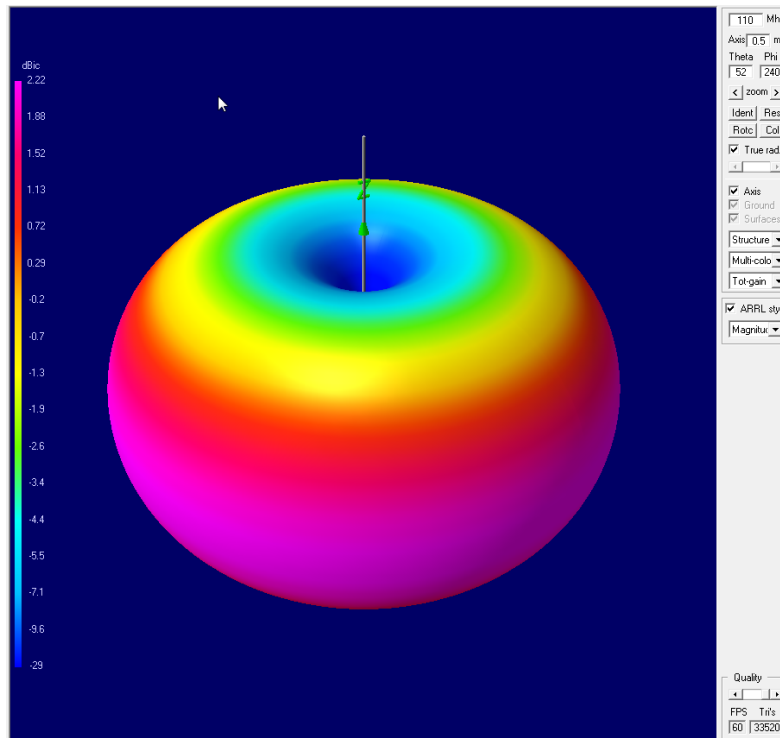


Figure 9. 3D dipole pattern at 110 MHz (modeled).

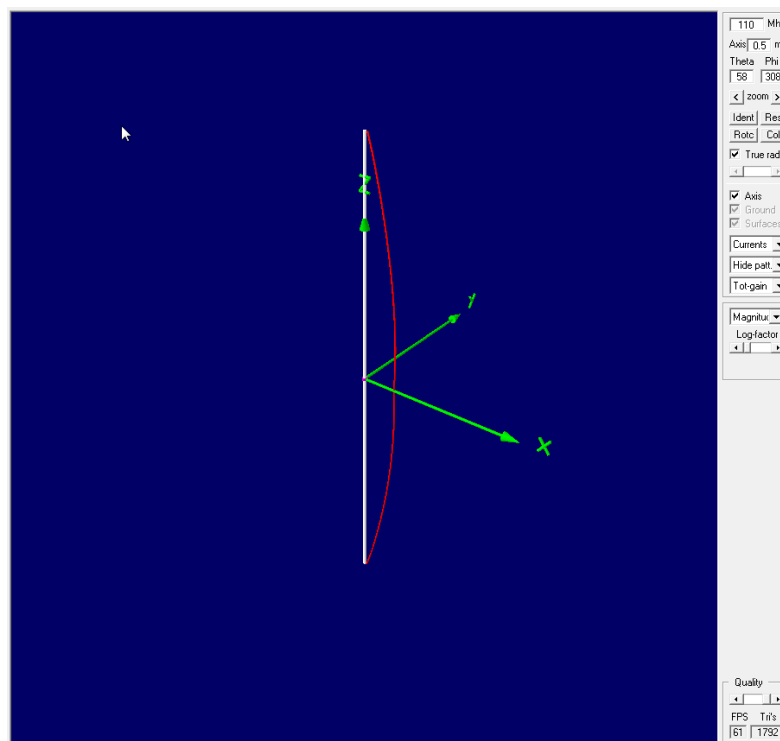


Figure 10. Dipole current distribution at 110 MHz (modeled).

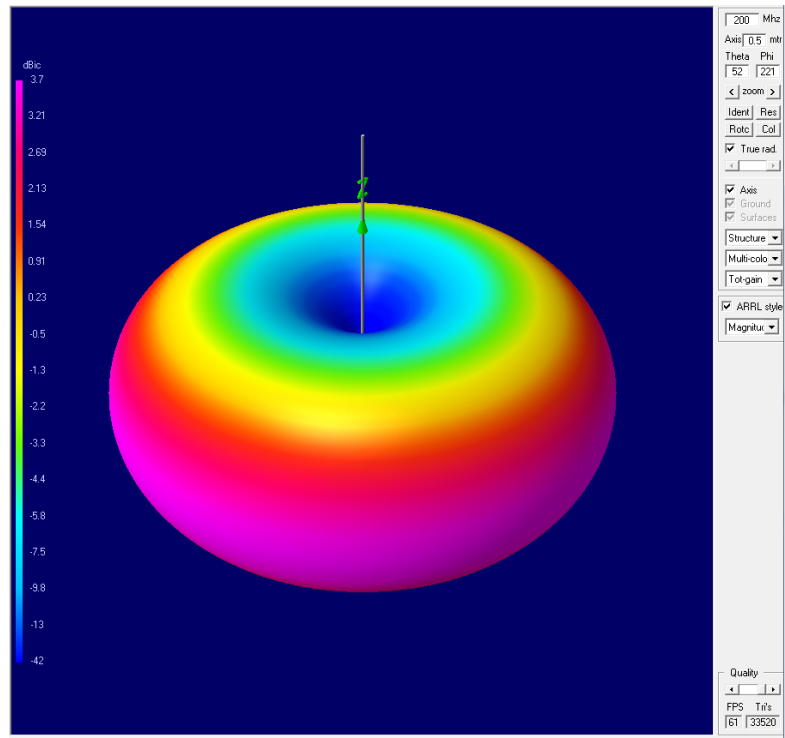


Figure 11. 3D dipole pattern at 200 MHz (modeled).

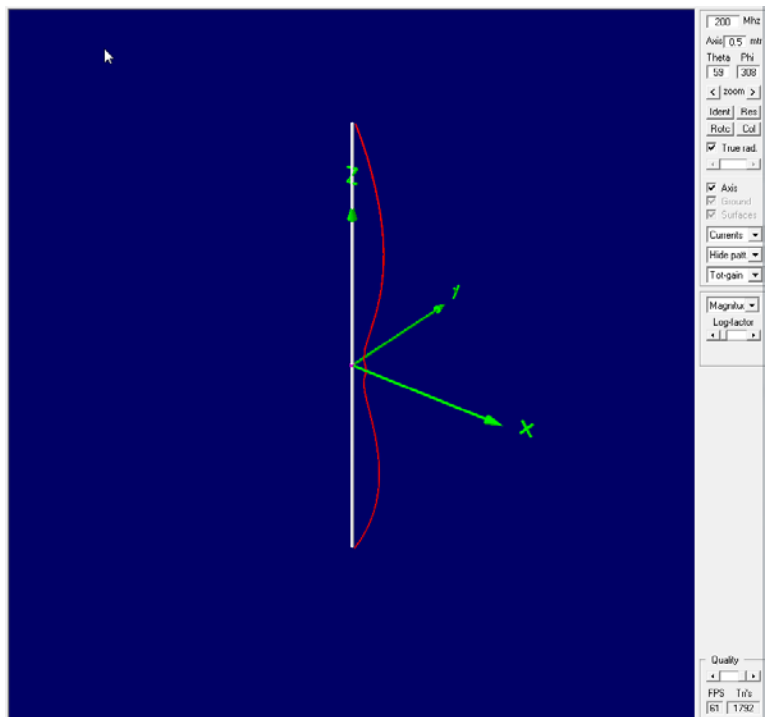


Figure 12. Dipole current distribution at 200 MHz (modeled).

The results from the model are typical and as expected for a $\lambda/2$ dipole over the frequency range of interest. The directivity, as inferred from the pattern, does not change much in the frequency range from 20 MHz to 110 MHz. A noticeable change in the pattern is observed at 200 MHz. The changes in pattern correspond to the changes in the current distribution along the antenna element. Two dimensional, vertical-plane, antenna patterns are shown in Figures 13 through 15.

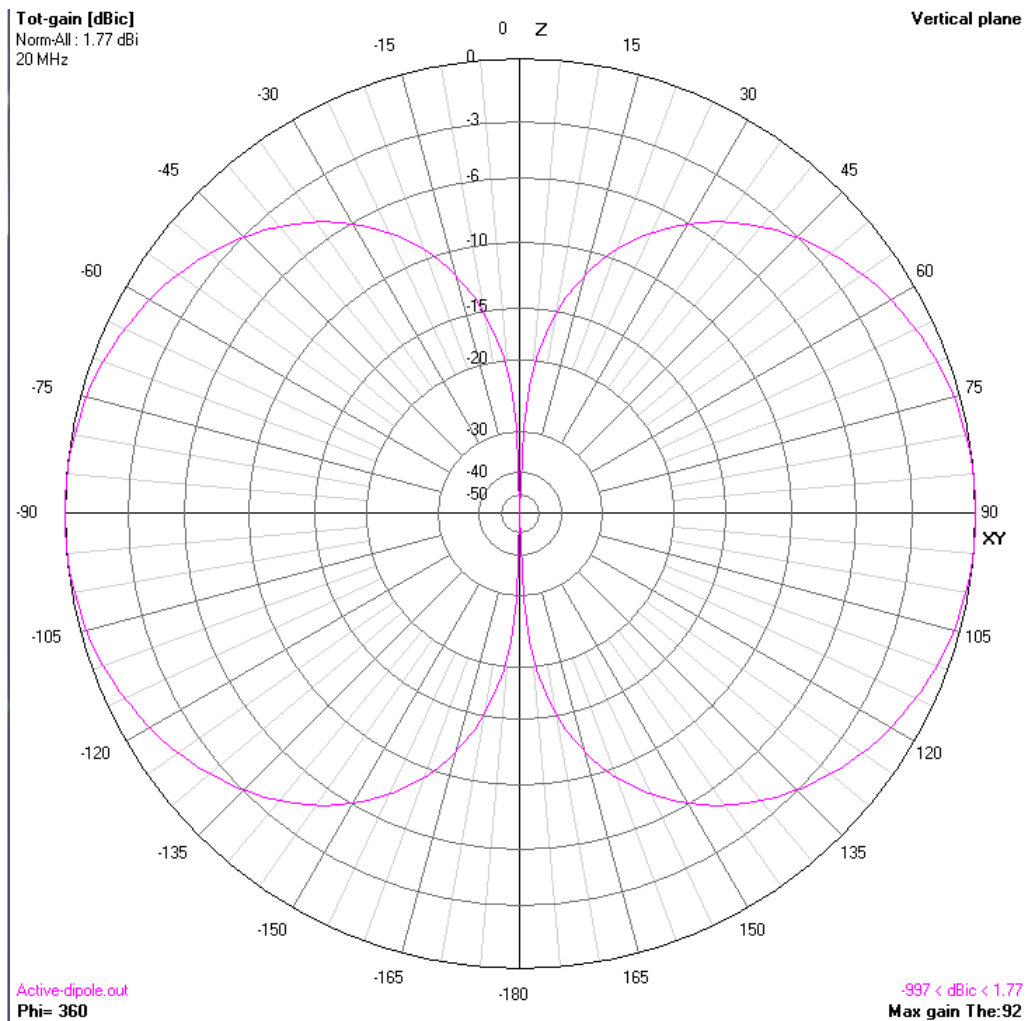


Figure 13. Vertical plane radiation pattern, $f(\theta)$, at 20 MHz (modeled).

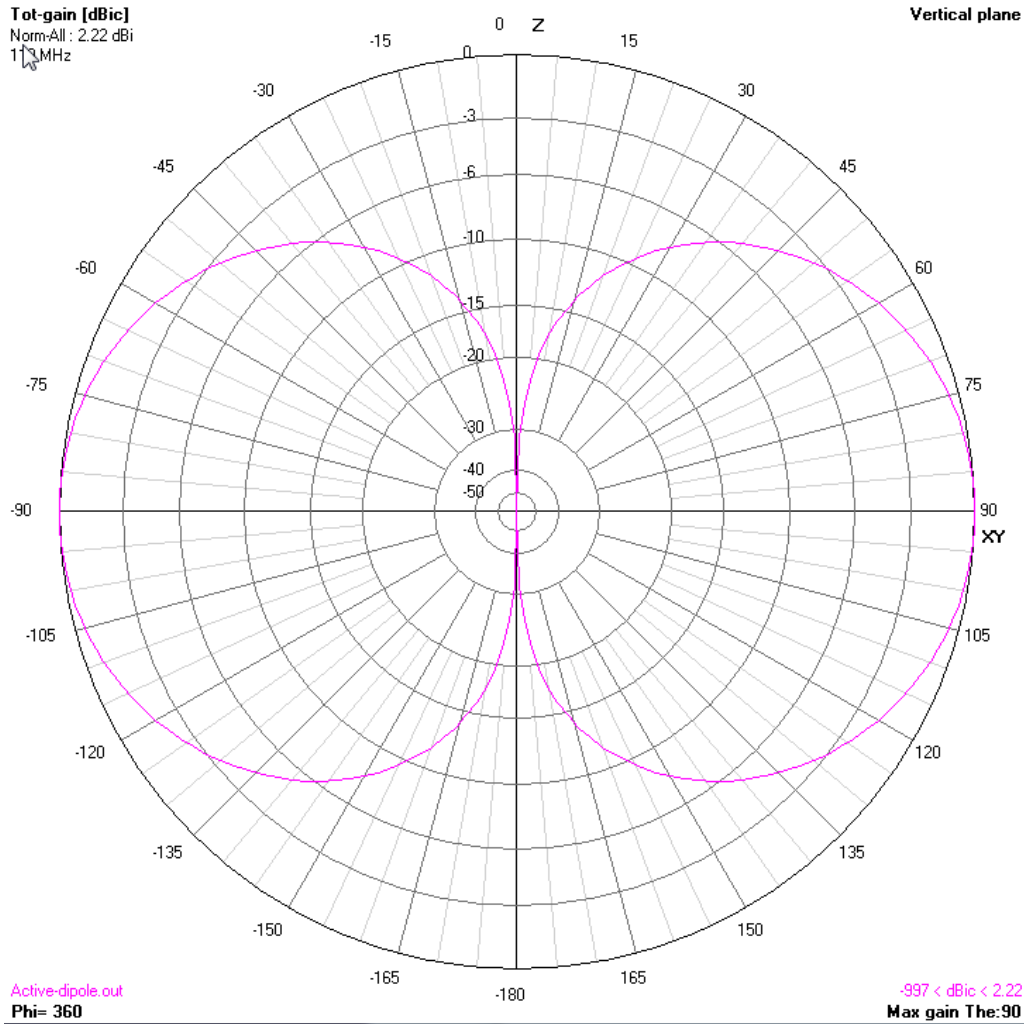


Figure 14. Vertical plane radiation pattern, $f(\theta)$, at 110 MHz (modeled).

The 3dB beam widths from the modeled data are shown in Table 1.

Table 1. Dipole 3 dB BW's (modeled).

Frequency	20 MHz	110 MHz	200 MHz
3 dB BW Modeled	88 deg.	76 deg.	48 deg.

These values match well with the theoretical 3 dB beam widths for a finite length dipole as defined in the literature [6,7].

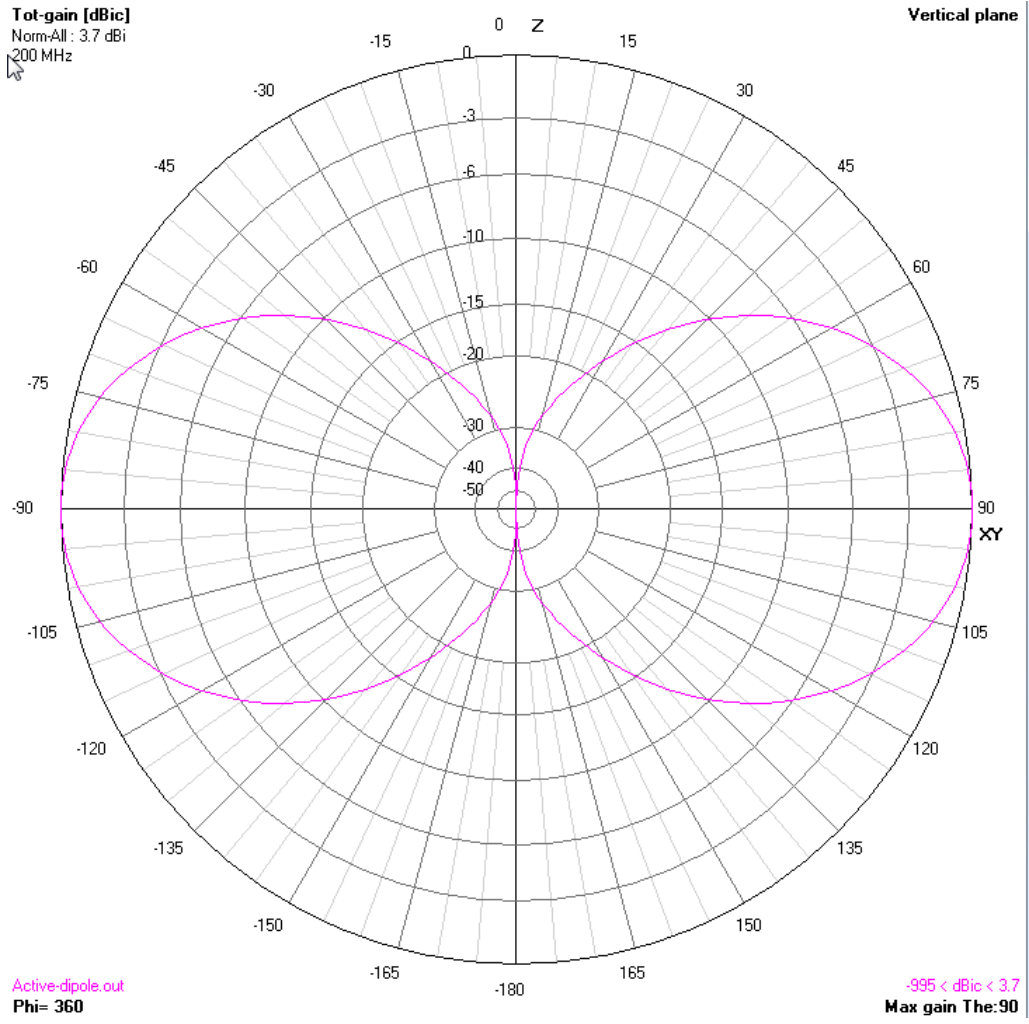


Figure 15. Vertical plane radiation pattern, $f(\theta)$, at 200 MHz (modeled).

The 4NEC2 model as implemented does not include any loss resistance, R_l . Therefore, the radiation efficiency reported at all frequencies is 100%. That is, with $R_l = 0$,

$$e_{cd} = R_r / (R_r + R_l) \tag{17}$$

reduces to

$$e_{cd} = R_r / R_r. \tag{18}$$

The radiation resistance values produced by the model are shown in Table 2.

Table 2. Dipole radiation resistance (modeled) as a function of frequency.

Frequency	Radiation Resistance (Ω)
20	1.62358
25	2.56726
30	3.7514
35	5.19581
40	6.92524
45	8.97017
50	11.3678
55	14.1633
60	17.4114
65	21.1787
70	25.546
75	30.6119
80	36.4974
85	43.3514
90	51.3585
95	60.7491
100	71.8128
105	84.9164
110	100.528
115	119.249
120	141.86
125	169.374
130	203.116
135	244.815
140	296.699
145	361.569
150	442.742
155	543.638
160	666.528
165	809.72
170	962.719
175	1101.31
180	1189.72
185	1197.45
190	1121.58
195	989.168
200	836.722

Based on this result, the antenna element gain is equivalent to the directivity, and is plotted in Figure 16.



Figure 16. Modeled gain at $\phi = 0$ and $\theta = 90$.

5.2.2 Element Implementation

In reality, there is a small, finite amount of loss resistance in the physical elements. This small amount of loss is difficult to measure, but it will have an impact on the radiation efficiency at the lower end of the frequency range where the loss resistance is proportionally larger relative to the radiation resistance.

The antenna elements selected for the prototype antenna were fabricated from 0.635 cm tubular brass stock. Two elements of 0.7 meters each were inserted into holes in the simple prototype housing. The ends of the elements inside the housing were spaced apart by a distance of 0.635 cm. The elements were then connected to the balun and amplifier PCB.

An engineering design unit, EDU, or a flight-ready antenna would use deployable antenna elements. Versions of deployable elements, with flight heritage are commercially available from aerospace vendors [13].

5.3 Amplifier and Balun PCB Design

The amplifier PCB houses both the low noise amplifier, LNA, and the balun transformer. The balun transformer is used to couple the balanced dipole elements to the unbalanced amplifier input transmission line. There will be an impedance mismatch between the antenna elements and the LNA. This mismatch will affect the reflection efficiency, e_r . This mismatch can be modified across the frequency band, but not eliminated [1,6,7]. The balun transformer can be used to transform the impedance, Z_{in} , between the elements and the amplifier, thus modifying the reflection efficiency.

$$e_r = (1 - |\Gamma|^2), \quad (19)$$

where

$$\Gamma = (Z_{in} - Z_0)/(Z_{in} + Z_0) \quad (20)$$

Z_{in} = radiation resistance (real part of antenna impedance)

$Z_0 = 50 \Omega$, load resistance (real part of load impedance).

The reflection efficiency expressed in dB is

$$e_r(dB) = 10 \log_{10}(e_r). \quad (21)$$

The reflection efficiency as a function of frequency and impedance transformation ratio is shown in Figure 17. These results are obtained by modifying the Z_{in} value by the transformation factor, which produces a change in the reflection coefficient.

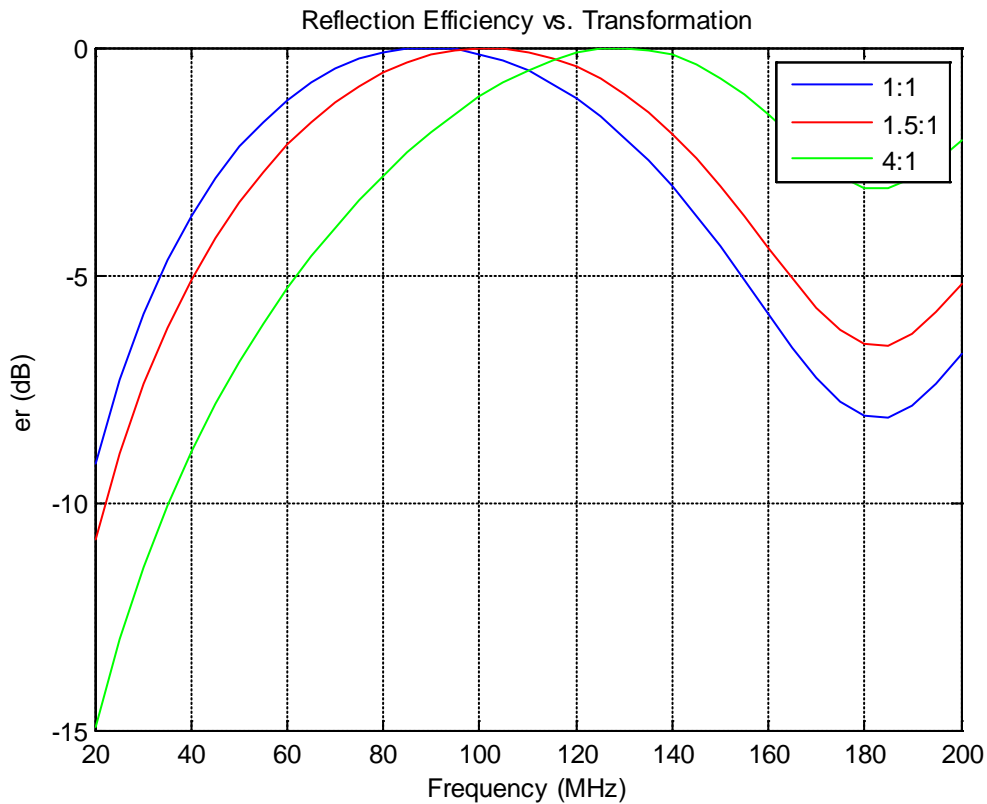


Figure 17. Reflection efficiency at various impedance transformations as a function of frequency.

The modification to the reflection efficiency manifests as a shift in frequency response. That is, an improvement in efficiency in one portion of the frequency band is offset by degradation in another portion of the frequency band. Therefore, there is no advantage in performing an impedance transformation, although the ‘balancing’ function of the balun transformer is still needed.

The balun selected is a 1:1 impedance ratio, commercially available surface mount component [14]. The surface mount configuration and small size of this balun make it appealing for the design.

The dipole gain after factoring in the reflection efficiency is shown in Figure 18.

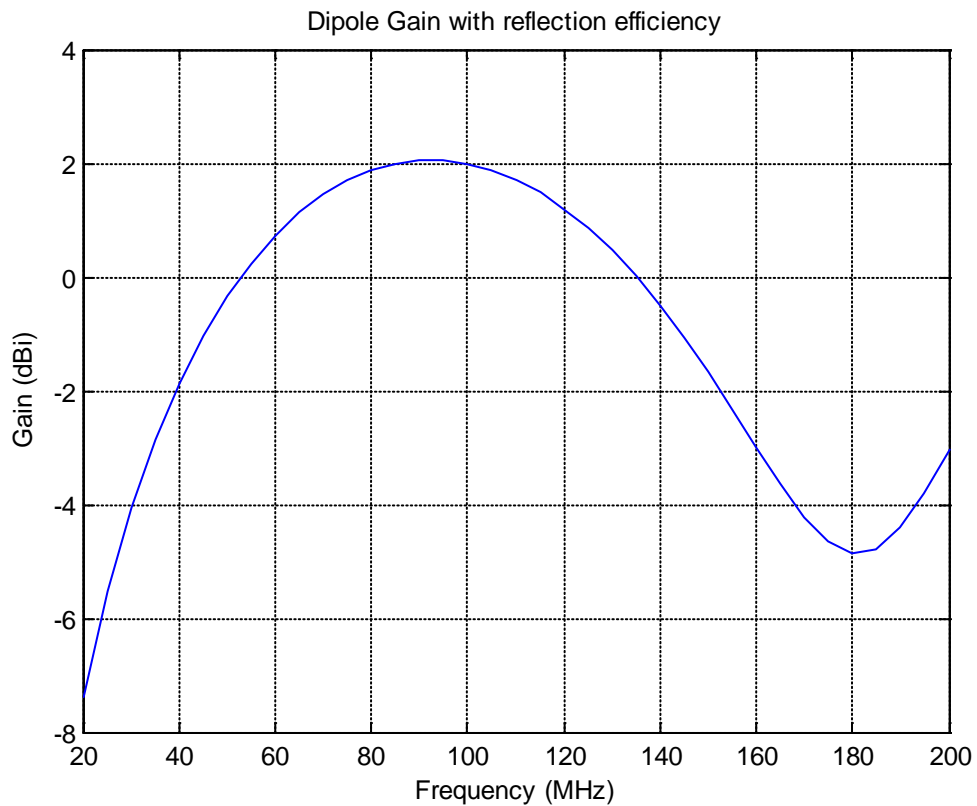


Figure 18. Dipole gain as a function of reflection efficiency and frequency.

For purposes of comparison, a model of a 3-element log periodic was constructed using the 4NEC2 software with the results shown in Figure 19. These results show that an improvement in bandwidth can be achieved with a more complex antenna design, but this approach would not provide the desired simplicity in design, and deployment.

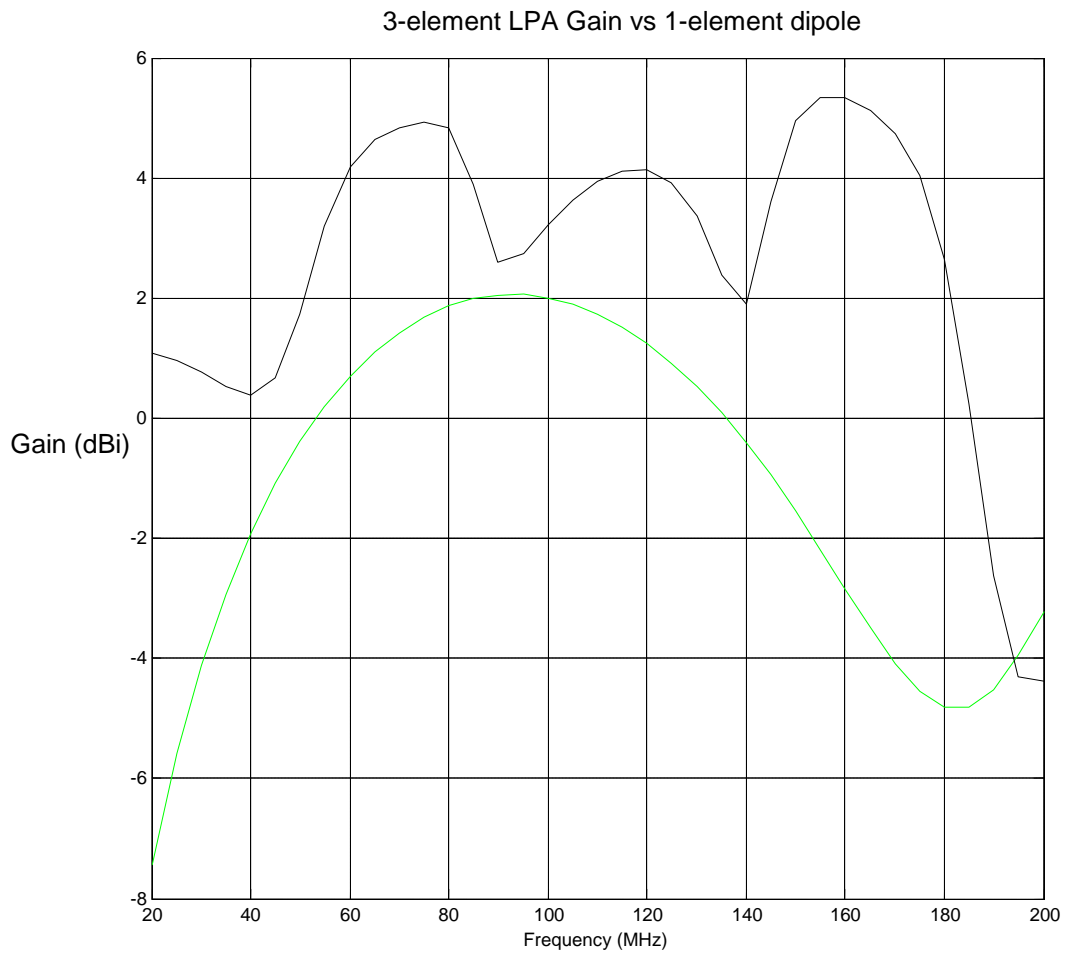


Figure 19. LPA and dipole bandwidth comparison, (gain as a function of frequency).

The amplifier component selected is a broadband, low-noise, 50 Ω , gain-block MMIC (monolithic microwave integrated circuit). This LNA presents an impedance of 50 Ω at its input and output. Matching between the leads of the MMIC and its internal, bipolar transistor is accomplished within the component and does not need to be addressed externally. Additionally, the stability of the LNA is addressed internally and does not require any external compensation over the frequency band of interest.

The particular LNA component being used in this design is Avago's MSA-0670 gain block. This component is usable in the frequency range of DC to 1 GHz [15]. The noise figure for the MSA-0670 in the frequency range of interest is listed as less than 2.8 dB.

The datasheet of this component indicates that it is unconditionally stable in the frequency range of our design. The component's S-parameters were verified at the frequencies of interest via network analyzer measurements. These results are shown in Table 3. The k and Delta values were calculated from the measured S-parameters using the appropriate equations discussed earlier in section 4.3.2.

Table 3. LNA MMIC S-parameters.

Frequency	S11 Mag	S11 ang	S21 Mag	S21 Ang	S12 Mag	S21 Ang	S22 Mag	S22 Ang	K	Delta
20 MHz	0.043	-150	9.4	-179	0.07	5.2	0.08	63	1.07	0.654
30 MHz	0.045	-176	9.4	-178	0.07	6	0.07	52	1.08	0.654
40 MHz	0.054	154	9.5	175	0.07	5.3	0.07	44	1.07	0.661
50 MHz	0.06	145	9.5	173	0.07	6.1	0.065	40	1.07	0.661
60 MHz	0.062	140	9.5	172	0.07	7.3	0.07	38	1.07	0.66
70 MHz	0.065	129	9.4	170	0.07	7.9	0.07	36	1.07	0.653
80 MHz	0.07	119	9.4	169	0.07	9.3	0.06	33	1.07	0.653
90 MHz	0.08	114	9.4	167	0.07	10.1	0.07	36	1.07	0.652
100 MHz	0.086	109	9.3	166	0.07	11.2	0.07	34	1.07	0.645
200 MHz	0.15	76	8.7	151	0.07	18.1	0.09	37	1.08	0.595

The expected gain of the combined amplifier and element responses as a function of frequency is shown in Figure 20.

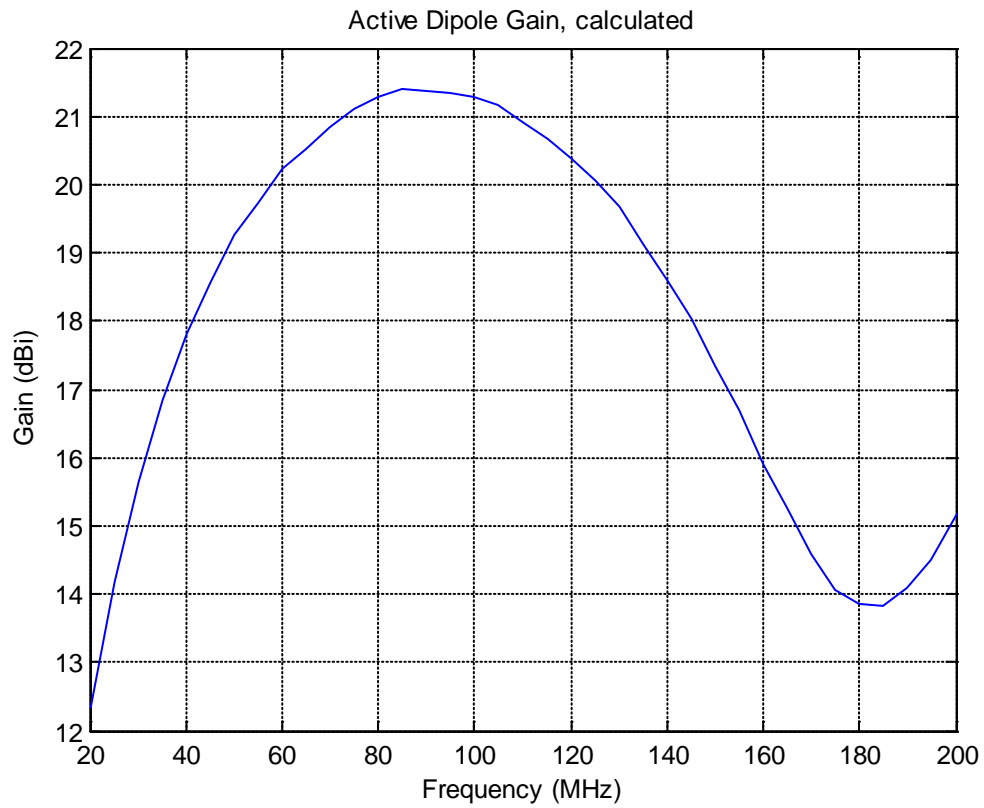


Figure 20 . Calculated complete antenna gain as a function of frequency.

The amplifier circuit was designed as specified in the datasheet, that is, with a bias current of 16 mA supplied by a 5 V source. The schematic diagram is shown in Figure 21.

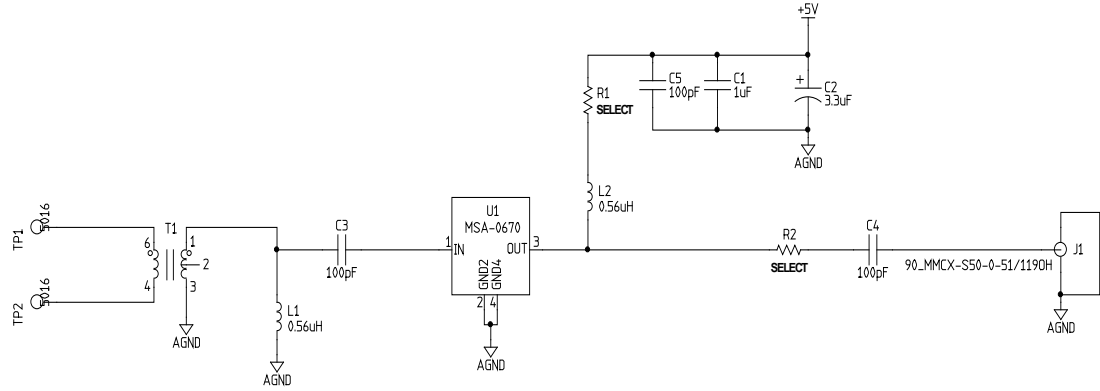


Figure 21. Schematic of the LNA with balun.

The bias resistor value was determined using

$$R_{bias} = V_{ss} - V_d / (I_{bias}), \quad (22)$$

where

$$V_{ss} = 5 \text{ V}$$

$$V_d = 3.5 \text{ V}$$

$$I_{bias} = 16 \text{ mA}.$$

The schematic includes DC blocking capacitors at the input and output. An inductor, functioning as an RF choke, is included in the biasing path to provide RF isolation between the voltage supply and the amplifier. Decoupling capacitors are also included in the biasing circuit to shunt any high frequency noise signals to ground.

5.3.1 PCB Implementation

The amplifier circuitry was accommodated on a PCB with an area of 11.43 cm². The PCB layout diagram is shown in Figure 22.

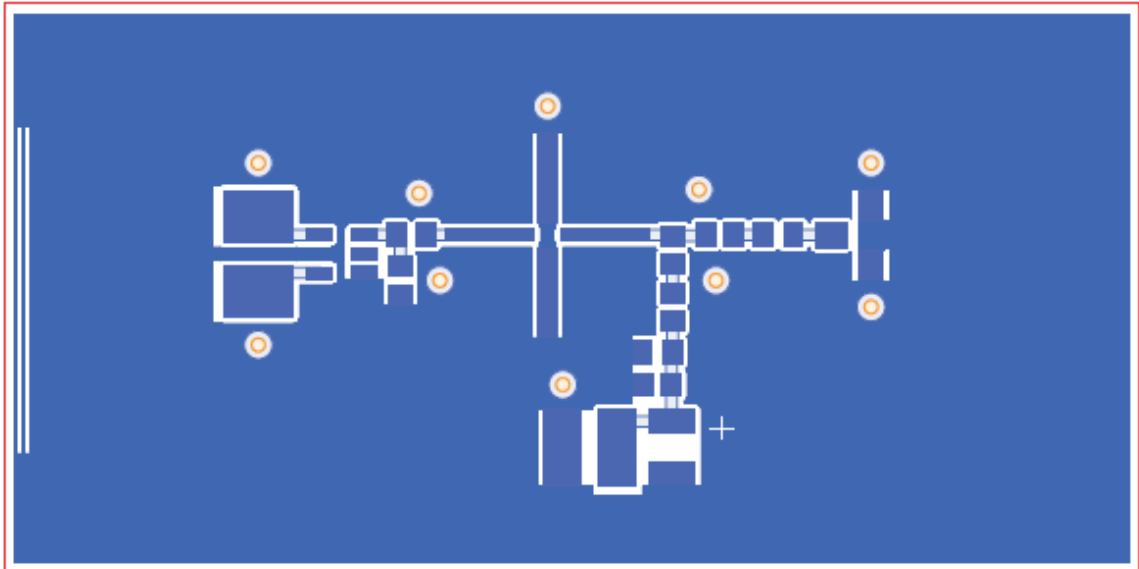


Figure 22. Layout artwork for the LNA PCB.

A photograph of the prototype amplifier PCB is shown in Figure 23.

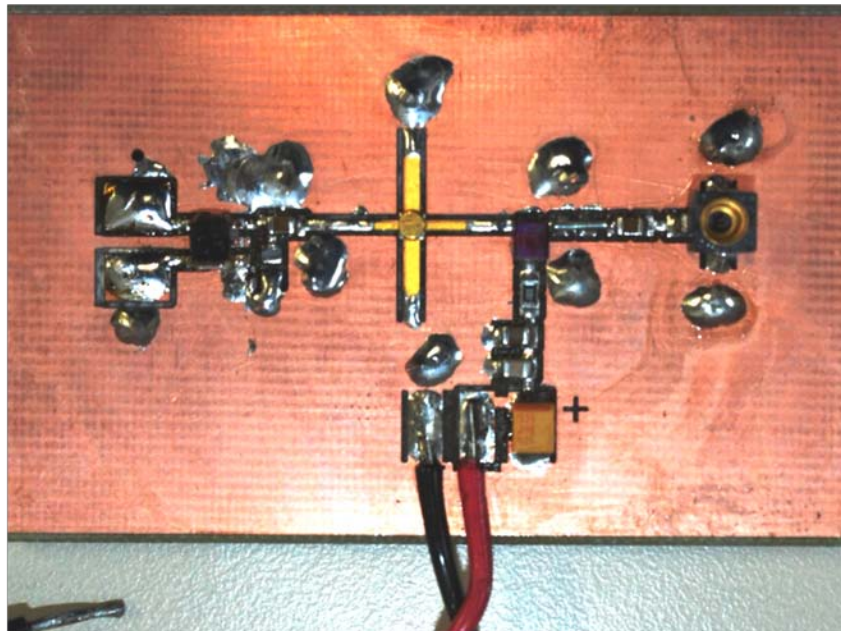


Figure 23. Photograph of the prototype LNA assembly.

A photograph of the prototype amplifier PCB installed in the prototype housing with the prototype elements attached is shown in Figure 24.



Figure 24. Photograph of the prototype active dipole installed in the prototype housing.

5.4 Housing Design

The prototype housing shown in Figure 24 is a simple plastic ring to which the antenna PCB is attached using a silicone based adhesive. The antenna elements are attached to the antenna PCB using short, large diameter conductors. The elements are inserted through access holes in the housing that provide a ‘tight’ fit around the elements to provide additional mechanical support to the elements. Photographs of the completed prototype antenna are shown in Figures 25 and 26.



Figure 25. Photograph of the full size prototype active dipole antenna.



Figure 26. Photograph of the active dipole antenna.

The EDU version of a housing to accommodate the PCB and undeployed antenna elements has a volume of 36 cm³. Mechanical drawings of the proposed housing are shown in Figures 27 and 28. The bottom of the housing is configured with mechanical standoff for mounting the PCB.

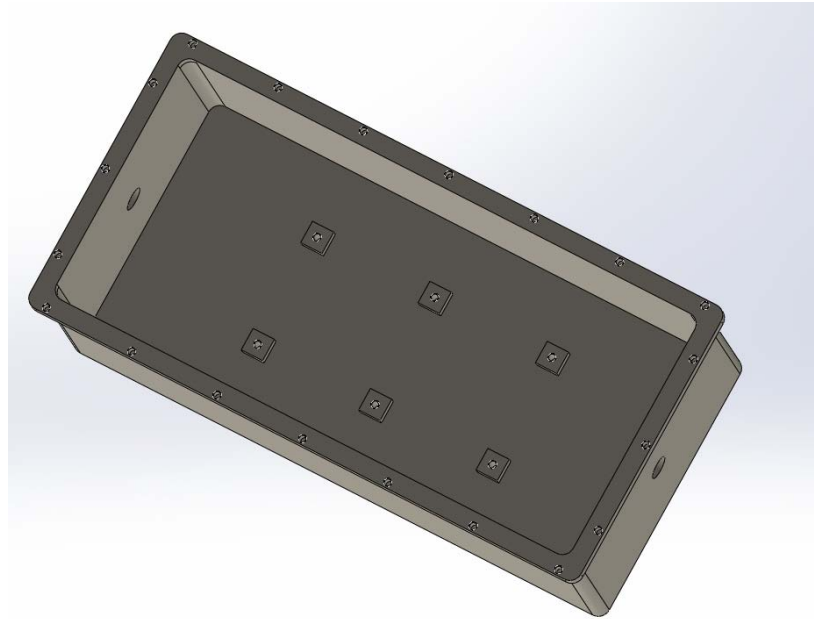


Figure 27. Drawing of the proposed EDU housing.

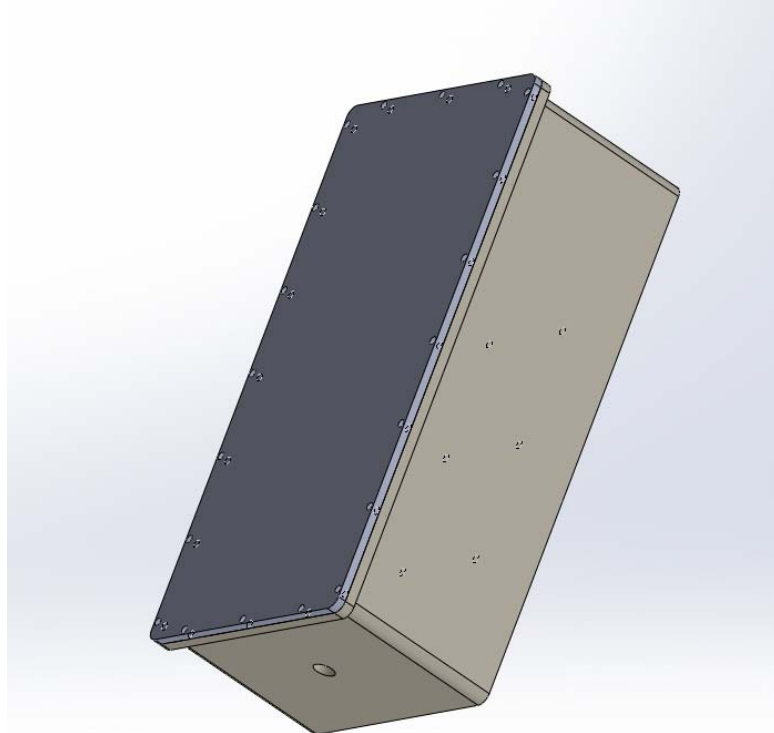


Figure 28. Drawing of the proposed EDU housing with cover.

After deployment, the antenna elements will be the largest part of the antenna, taking up a space of 1.4 meter in length. The dimensions of the volume envelope taken up by the antenna are 5 cm x 7.6 cm x 1.4 m. A drawing of the conceptual design is shown in Figure 29.

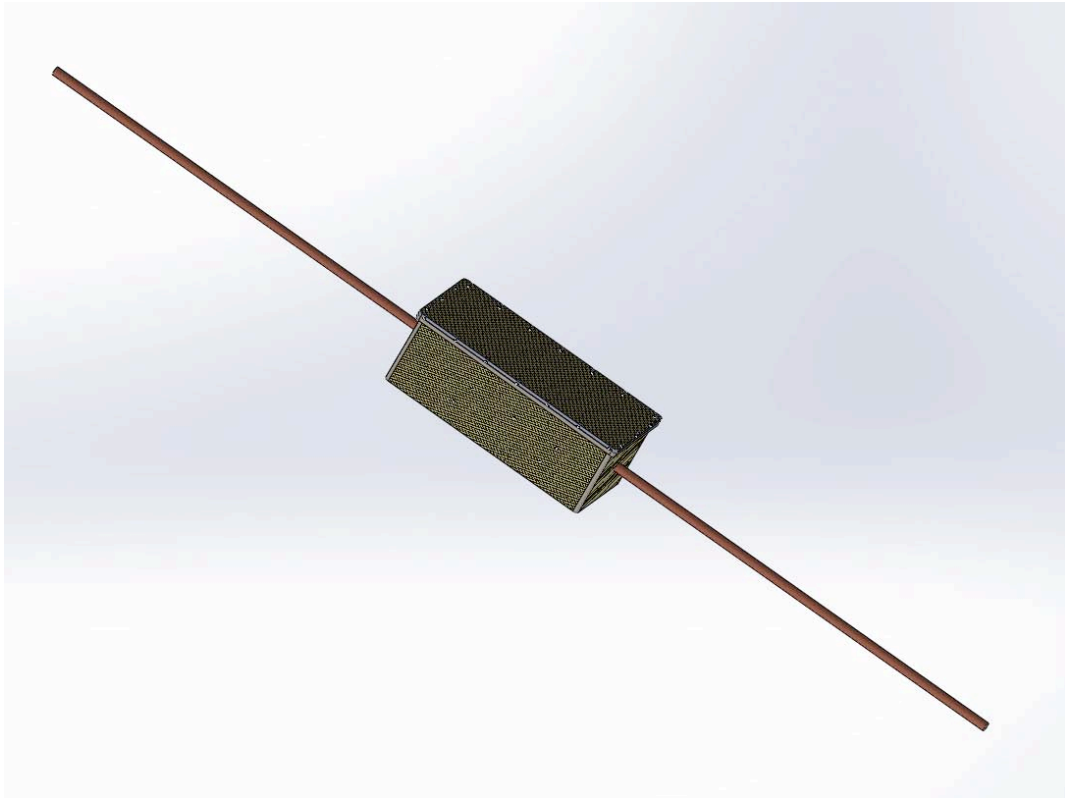


Figure 29. Drawing of the proposed EDU active dipole.

5.5 Summary of Chapter 5

In this chapter the design and implementation of the complete antenna was presented. The element and amplifier components were discussed. The design of each of these components was discussed and anticipated performance was presented. The anticipated performance was based on calculations and modeling.

The implementation of the design was presented through the use of schematics, layout drawings and photographs of the completed prototype assemblies. Additionally, a proposed implementation of an EDU design was provided in the form of mechanical drawings.

Chapter 6

6.1 Test and Verification

The gain of the stand alone LNA as well as the overall gain of the completed antenna were measured. The results of those measurements are presented in the following sections.

6.1.1 Amplifier Measurements

Complete S-parameter measurements were taken and were used in the stability calculations discussed in the previous chapter. The specific amplifier gain or forward gain is taken from the S_{21} S-parameter. The amplifier gain in dB is calculated using

$$G_{dB} = 20 \log_{10} |S_{21}| \quad (23)$$

and is shown in Table 4 and plotted in Figure 30.

Table 4 LNA gain (measured) as a function of frequency.

Frequency	Gain dB
20 MHz	19.4626
30 MHz	19.4626
40 MHz	19.5545
50 MHz	19.5545
60 MHz	19.5545
70 MHz	19.4626
80 MHz	19.4626
90 MHz	19.4626
100 MHz	19.3697
200 MHz	18.7904

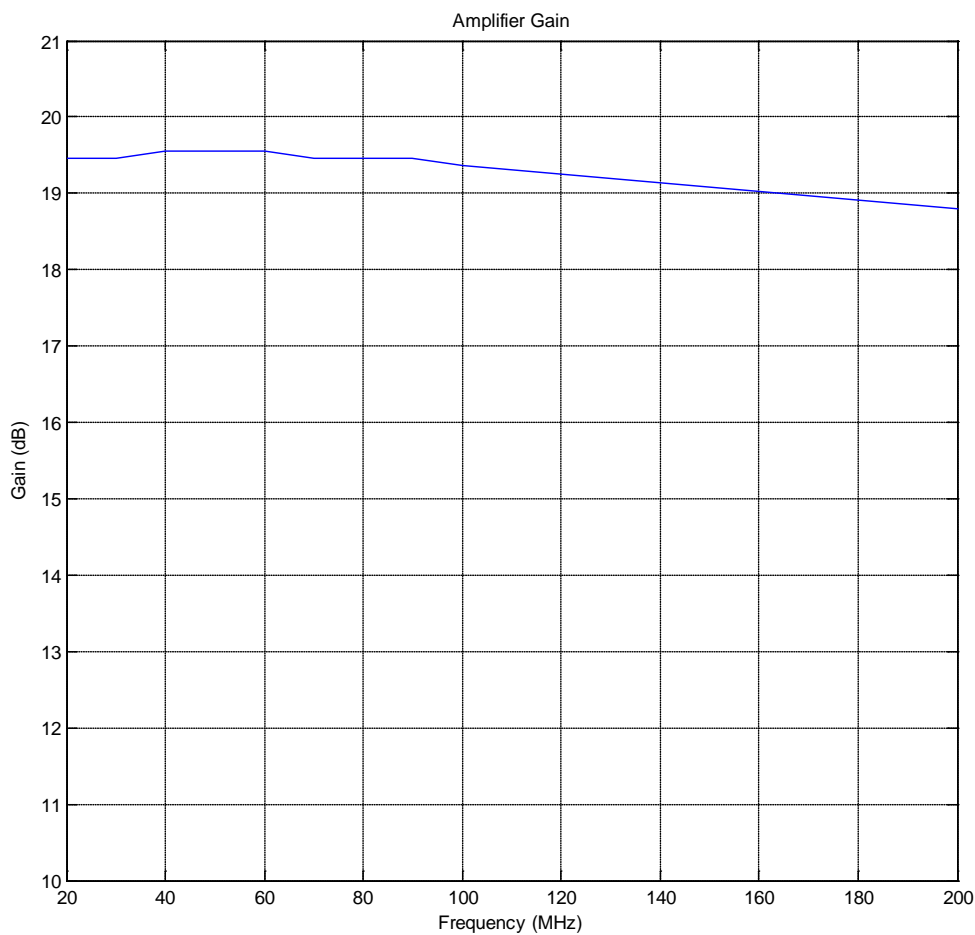


Figure 30. Measured LNA gain as a function of frequency.

6.1.2 Antenna Gain Measurements

Gain measurements of the antenna were performed in an anechoic test chamber. The measurement was a comparative measurement relative to zero calibration using two bicone antennas operating in the same frequency range [16]. That is, two bicone antennas were placed in the test chamber at a separation of 3.2 meters. The antennas were connected to an Agilent network analyzer configured for an S_{21} response measurement. A

response calibration was performed to effectively produce a 0 dB reference. The separation distance used ensures that the test antenna will be in the far field r_{ff} per [6,7]

$$r_{ff} = 2D^2/\lambda \quad (24)$$

with

$D = 1.4$ meters (largest dimension of test antenna under test).

The 3.2 meter distance was determined to be more than sufficient based on the results of the far field calculation over the frequency band of interest, which are shown in Table 5.

Table 5 Calculated far field distances as a function of frequency.

Frequency	Far Field (meters)
20 MHz	0.2613
30 MHz	0.392
40 MHz	0.5227
50 MHz	0.6533
60 MHz	0.784
70 MHz	0.9147
80 MHz	1.0453
90 MHz	1.176
100 MHz	1.3067
200 MHz	2.6133

The antenna gain was measured only at bore sight, i.e., $\theta=90$ and $\Phi=0$. Full elevation and azimuth patterns were not taken. The gain results are shown in Figure 31.

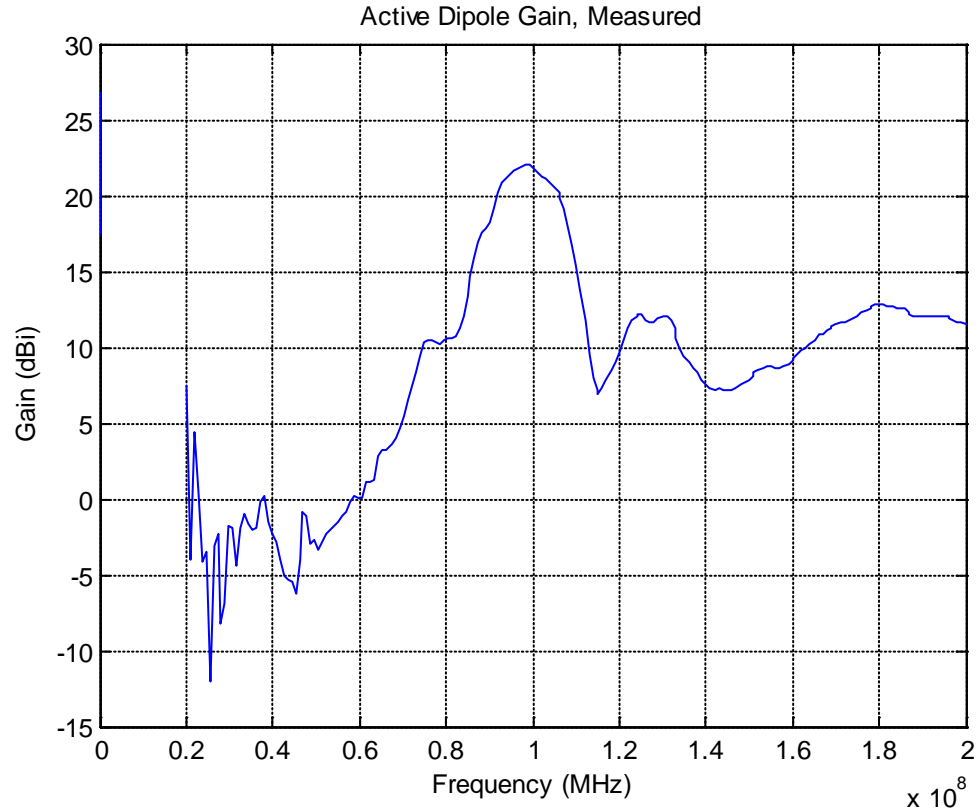


Figure 31. Measured completed active antenna gain as a function of frequency.

The measured antenna gain shows the expected higher gain at $\lambda/2$ relative frequency, as was also indicated in the model. The measured peak gain is equivalent to the peak gain calculated from the model. The 3 dB frequency bandwidth, relative to the peak gain, is narrower in the measured data than in the modeled result. The overall minimum to maximum delta is also larger in the measured result than in the modeled result. These deviations from the modeled result are attributable to subtle differences that arose during implementation of the design in addition to variables in the measurement setup.

6.2 Summary of Chapter 6

In Chapter 6, the results of the measurement performed on the amplifier and completed antenna were presented. A comparison between the modeled and measured results was presented.

Chapter 7

7.1 Conclusions

An active dipole antenna design provides a flexible solution to meet the requirements of a space vehicle hosted antenna. The omni-directional pattern of the dipole provides a broad field of view that can fit the needs of many types of missions. The small physical envelope of the completed antenna can easily fit into many vehicle designs. The few-component, MMIC based amplifier design provides a low risk, reliable solution for improving antenna gain, while consuming a minimal amount of power.

The active dipole antenna design does not necessarily meet the highly detailed, very specific needs of every mission type and is not the optimal solution for every application. It does, however, meet the needs of many missions by providing a general purpose alternative that is simple in design and that can be easily integrated into many different applications.

The physical design of the EDU antenna with a rigid housing and surface mount PCB is robust and poses low risk with regards to vibration. The design of the EDU housing also allows for introduction of radiation shielding if needed.

7.1.1 Scaling

Pseudo frequency requirements were imposed on the design as a point of reference for the design development. However, the active dipole concept presented, i.e., dipole

elements and MMIC LNA, can be implemented in other frequency ranges through simple antenna element scaling and proper selection of LNA.

7.2 Path Forward

Further work on this particular design would include completion of an EDU level antenna, including gain and pattern measurements. Investigation of the behavior of the antenna pattern as a function of location on and proximity to the SV need to be performed using the 4NEC2 modeling software.

The active antenna design as proposed can be thought of as a single dipole “unit” or “block”. These basic building blocks can be configured into an array of dipoles. The array of dipoles can either be linearly or circularly polarized. The behavior that arises from combining antenna blocks into various configurations needs to be modeled.

Investigations into the gain and phase relationships between individual antenna blocks within an array would yield interesting results. The subtleties in the active circuitry and degradation of components over time need to be investigated and understood as part of pursuing an active array design.

References

- [1] J.D. Krauss and R.J. Marhefka, “Antennas for All Applications, Third Edition”, McGraw-Hill, 2003
- [2] J. Wertz, D. Everett, J. Puschell, “Space Mission Engineering: The New SMAD”, *Microcosm Press*, Hawthorne, CA, 2011.
- [3] Hosted Payloads. (2011) Hosted Payloads. [Online]. Available at: <http://www.space.commerce.gov/general/commercialpurchase/hostedpayloads.shtml> (Accessed: 10 October 2012).
- [4] 1U Cubesat kit chasis. [Online] Available at: <http://www.cubesatkit.com/docs/cubesatkitflyer.pdf> (Accessed: 10 November 2012).
- [5] Ncube-2, a Norwegian Cubesat. [Online] Available at: <http://en.wikipedia.org/wiki/CubeSat> (Accessed: 10 October 2012)
- [6] C. A. Balanis, “Antenna Theory Analysis and Design 3rd Ed”, *John Wiley & Sons*, Hoboken, NJ, 2005.
- [7] J. D. Krauss, “Antennas, Second Edition”, McGraw-Hill, 1988.
- [8] F. Chen, “Plasma Physics and Controlled Fusion, Second Edition”, Plenum Press, New York, NY, 1984
- [9] D. Pozar, “Microwave Engineering, Third Edition”, John Wiley and Sons, Hoboken NJ, 2005.
- [10] A. Voors, “4NEC2, NEC Based Antenna Modeler and Optimizer.” [Online]. Available at: <http://home.ict.nl/~arivoors/> (Accessed: 9 February 2012).
- [11] G. Gonzales, “Microwave Transistor Amplifiers, Analysis and Design, Second Edition”, Prentice Hall, Inc., Upper Saddle River, NJ, 1997.
- [12] S. Erst, “Receiving System Design”, Artech House, Norwood, MA, 1984.
- [13] Stem JIB Antenna, Northrup Grumman Space Technology, Astro Aerospace, Carpinteria, CA

- [14] Surface Mount RF Transformer, TC1-1TX+, Minicircuits, Brooklyn, NY
- [15] MSA-0670 Cascadable Silicon Bipolar MMIC Amplifier, Avago Technologies, San Jose, CA
- [16] SAS-544 Biconical Antenna Operation Manual, A.H. Systems Inc. May, 2006